Structure of Poly(styrene-*b*-ethylene-*alt*-propylene) Diblock Copolymer Micelles in Squalane[†]

Soo-Hyung Choi,[‡] Frank S. Bates,*[,‡] and Timothy P. Lodge*[,‡,§]

Department of Chemical Engineering and Materials Science and Department of Chemistry, University of Minnesota, Minneapolis, Minnesota 55455

Received: December 16, 2008; Revised Manuscript Received: February 11, 2009

The temperature dependence of the micellar structures formed by poly(styrene-*b*-ethylene-*alt*-propylene) (SEP) diblock copolymers in squalane, a highly selective solvent for the PEP blocks, has been studied using dynamic light scattering (DLS) and small-angle X-ray scattering (SAXS). Four SEP diblock copolymers were prepared by sequential anionic polymerization of styrene and isoprene, followed by hydrogenation of the isoprene blocks, to yield SEP(17−73), SEP(26−66), SEP(36−69), and SEP(42−60), where the numbers indicate block molecular weights in kDa. All four polymers formed well-defined spherical micelles. In dilute solution, DLS provided the temperature-dependent mean hydrodynamic radius, R_h, and its distribution, while detailed fitting of the SAXS profiles gave the core radius, R_c, the equivalent hard sphere radius, R_{hs}, and an estimate of the aggregation number, N_{agg}. In general, the micelles became smaller as the critical micelle temperature (CMT) was approached, which was well above the glass transition of the core block. As concentration increased the micelles packed onto body centered cubic lattices for all four copolymers, which underwent order−disorder transitions upon heating near the dilute solution CMTs. The results are discussed in terms of current understanding of block copolymer solution self-assembly, and particular attention is paid to the issue of equilibration, given the high glass transition temperature of the core block.

Introduction

Block copolymers can self-assemble into micelles in selective solvents. Typically, micelles consist of a compact core of insoluble blocks and a swollen corona of soluble blocks. Three free energy terms contribute to determining the micelle structure: the interfacial tension between the solvent and the core block, chain stretching of the core, and excluded volume interactions between the solvated corona blocks. Extensive reviews of the theory and experimental results describing these systems are available.[1−3] Micellar structures in selective solvents (both aqueous and organic) has been studied using small-angle neutron or X-ray scattering (SANS or SAXS), in combination with detailed fitting models.[4−20] In most of these studies, temperature was a key parameter to change solvent selectivity, which leads to changes in micellar properties. Most of the authors cited above have used a low glass transition temperature (T_g) material as the core block, such as poly(isoprene) (PI), poly(ethylene-*alt*-propylene) (PEP), poly(propylene oxide) (PPO), and poly(butylene oxide) (PBO), to avoid complications resulting from kinetically frozen dispersed micelles. However, even glassy polymers such as polystyrene (PS) will experience a reduction in T_g when immersed in a nonsolvent; for example, T_g of the PS blocks in PS-PI micelles in tetradecane is reported to be less than 40 °C because of solvent penetration into the core.[21]

While most investigations dealing with block copolymers dispersed in a selective solvent have attempted to focus on an equilibrium state of molecular assembly, nonequilibrium effects are ubiquitous and have been attributed either to a glassy core, a low critical micelle concentration (CMC), or both. Well-studied examples of the latter phenomenon can be found in the class of amphiphilic diblocks comprised of poly(ethylene oxide) (PEO) and any of a variety of hydrocarbon polymers including poly(butadiene) (PB) and PEP.[22−24] When dispersed in water at concentrations up to about 10% by weight, PB-PEO and PEP-PEO diblocks produce nonergodic dispersions that exhibit no measurable chain exchange, notwithstanding a core T_g well below the experimental temperature. This result can be traced to the extreme thermodynamic incompatibility between the organic core blocks and the aqueous medium.

Increasing the core T_g introduces a second type of complication. In this situation the micelle shape and dimensions reflect a state of assembly established at a higher temperature and subsequently frozen upon cooling. A glassy core resists both block copolymer exchange and micelle-micelle interactions such as coalescence. Nonequilibrium structures, prepared at low temperatures, may transform through full or partial equilibration upon heating above T_g, leading to a new state of organization that is locked in place with cooling. The shape and dimensions of the micelle core and corona can be characterized by small-angle X-ray and neutron scattering (SAXS and SANS), dynamic light scattering (DLS), dynamic mechanical spectroscopy (DMA) and other rheological measurements, and cryogenic transmission electron microscopy (cryo-TEM). In general several of these techniques are required to establish the structural and dynamical features that govern a particular micellar dispersion.

This report focuses on the structure of sphere-forming poly(styrene-*b*-ethylene-*alt*-propylene) (PS-PEP or SEP) diblock copolymers in squalane, a highly selective solvent for the PEP blocks (Figure 1). DLS and synchrotron SAXS, conducted between 35 and 190 °C, have catalogued the structure of four SEP systems characterized by differing molecular weights and compositions, both above and below the PS core glass transition

[†] Part of the "H. Ted Davis Special Section".

* To whom correspondence should be addressed. E-mail: bates@cems.umn.edu, lodge@umn.edu.

[‡] Department of Chemical Engineering and Materials Science.

[§] Department of Chemistry.

10.1021/jp8111149 CCC: $40.75
Published on Web 03/25/2009

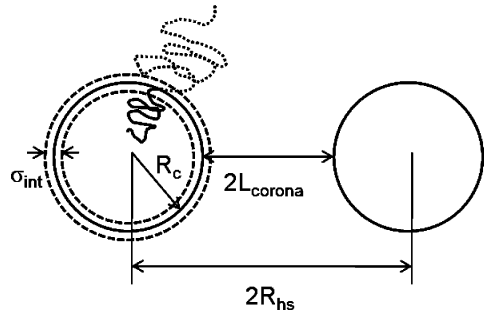

Figure 1. Schematic drawing of diblock copolymer micelle.

temperature. Previously, Quintana et al. deduced based on light scattering[25,26] that the micellar properties of SEP in *n*-alkane solvents ($n \leq 16$) become less dependent on temperature (up to 85 °C) with increasing *n*. This was attributed to the associated increase in T_g with *n*, which results from a decrease in solvent quality. Our choice of squalane ($n = 30$) as a solvent avoids this complication while affording access to a wide range of experimental temperatures. In this way we have been able to investigate the transition from nonequilibrium to equilibrium behavior in SEP micelles over the aforementioned range of temperatures. Our findings shed new light on the fascinating and technologically important topic of block copolymer micellization in selective solvents.

Experimental Section

Materials. Four poly(styrene-*b*-ethylene-*alt*-propylene) (SEP) diblock copolymers were synthesized via anionic polymerization of poly(styrene-*b*-isoprene) (SI), followed by selective hydrogenation of the polyisoprene block. Isoprene and styrene were polymerized sequentially by standard anionic polymerization procedures.[27] Isoprene and styrene were purified with *n*-butyl lithium and dibutyl magnesium for 4 h, respectively. Cyclohexane was used as the solvent and purified by passing through a purification column. Using *sec*-butyl lithium as an initiator, the isoprene was polymerized for 8 h at 40 °C, followed by the addition of styrene and polymerization for 8 h at the same temperature.

SI diblock copolymers were selectively hydrogenated using a homogeneous Ni−Al catalyst.[28] A polymer solution was prepared by dissolving 10 g of SI polymer in 500 mL of purified cyclohexane, which was added to a 1 L stainless steel hydrogenation reactor. A catalyst solution was prepared by injecting 6 mL of triethylaluminum (Sigma-Aldrich) into stirred 20 mL of 0.1 M nickel 2-ethylhexanoate (Sigma-Aldrich) in cyclohexane under argon. After adding the catalyst solution to the hydrogenation reactor, the reactor was charged with high purity hydrogen (∼300−400 psi) at a temperature of 77 °C for at least 24 h. SEP polymer was recovered by stirring with 1000 mL of 8 wt% aqueous citric acid until the catalyst color disappeared, followed by filtration with activated alumina and precipitation from methanol.

The polymers were characterized by size exclusion chromatography (SEC, Waters) using a refractive index detector, and by ^{1}H nuclear magnetic resonance spectroscopy (^{1}H NMR, Varian Inova 300). Number average molecular weights (M_n) were determined using a combination of SEC and ^{1}H NMR. A small aliquot of PS was removed from the reactor prior to addition of isoprene, and characterized by SEC (calibrated with PS standards). ^{1}H NMR was used to determine the mole fraction of 4,1-addition in the PI block (94 ± 1%) and to determine the volume fraction of each block, assuming densities of 1.047 and 0.913 g/cm^3 for PS and PI, respectively. From these two quantities we calculated the overall M_n. Diblock polydispersities were estimated from the SI SEC curves. ^{1}H NMR also was employed to establish the extent of PI saturation, which in all cases was greater than 99%. The characteristics of the four SEP polymers in this study are shown in Table 1. The polymer name refers to SEP diblock copolymers with the PS and unsaturated PI molecular weight (kg/mol).

TABLE 1: Sample Characteristics

samples	PS block M_n (kg/mol)[a]	PI blockM_n (kg/mol)[b]	N_{PS}[c]	N_{PEP}[d]	M_w/M_n	f_{PS}[e]
SEP(42−60)	42	60	400	880	1.04	0.38
SEP(36−69)	36	69	350	1020	1.03	0.31
SEP(26−66)	26	66	250	970	1.04	0.26
SEP(17−73)	17	73	170	1070	1.04	0.17

[a] Number-average molecular weight of PS block is based on $M_{n,PI}$ and the composition determined by ^{1}H NMR. [b] Number-average molecular weight of PI block before hydrogenation determined by SEC based on polystyrene standards. [c] Number of monomer repeat units in PS block. [d] Number of monomer repeat units in PEP block. [e] Volume fraction of PS block in diblock copolymer.

Polymer solutions were prepared gravimetrically using methylene chloride as a cosolvent. The solvent, squalane (Sigma-Aldrich), was used as received. The cosolvent was removed at room temperature until constant weight was achieved.

Dynamic Light Scattering (DLS). Dynamic light scattering was utilized to determine the micelle hydrodynamic radius (R_h) as a function of temperature. The polymer solutions were filtered through 0.2 μm filters to remove dust, and sealed in 0.25 in. tubes under vacuum. The solutions were investigated using home-built goniometer equipped with a silicon oil index-matching bath, an electric heater, a Brookhaven BI-DS photomultiplier, a Lexel 95−2 Ar^+ laser operating at 488 nm and a Brookhaven BI-9000 correlator. The intensity autocorrelation function, $g^{(2)}(q,t)$, was typically measured at an angle of 90°. The cumulant method was used to obtain an average decay rate ($\bar{\Gamma}$) and the second cumulant (μ_2) which, when appropriately normalized, is a measure of the relative width of the distribution ($\mu_2/\bar{\Gamma}^2$).[29] The corresponding R_h is then calculated via the Stokes−Einstein equation

$$R_h = \frac{kT}{6\pi\eta_s D_0} \quad (1)$$

where *k*, *T*, η_s, and D_0 ($= \bar{\Gamma}/q^2$, where *q* is the scattering wave vector) are the Boltzmann constant, absolute temperature, solvent viscosity, and diffusion coefficient, respectively.

Small-Angle X-ray Scattering (SAXS). Small-angle X-ray scattering was performed using beam line 5ID-D, in the DuPont-Northwestern-Dow (DND-CAT) station at the Advanced Photon Source, Argonne National Laboratory. Radiation of 14 keV, corresponding to a wavelength $\lambda = 0.8856$ Å, was selected from an undulator beam using a double-crystal monochromator, and the sample to detector distance was 5.47 m. 2-D SAXS images were collected using a MAR-CCD detector. Temperature was controlled by an electric heater under a slightly positive pressure of helium. The samples were prepared by sealing in capillary tubes. Dilute solutions were preannealed at 190 °C for at least five hours. Experiments were performed by annealing samples at the selected temperature for at least four minutes, followed by X-ray exposure for 2−20 s. The sample temperature was increased from room temperature to 190 °C, and then decreased to room temperature, by 15−20 degree intervals.

The images were azimuthally averaged to the one-dimensional form of intensity versus wavevector $I(q)$ using the data reduction software FIT2D. The solvent background was also collected and subtracted from the solution data. The resulting data were not adjusted to an absolute scale. The reduced data of 1 wt% samples were analyzed with a fitting model described below, using IGOR Pro.

Fitting Model. The scattering form factor for a micelle consisting of a spherical core and Gaussian corona chains attached to the core surface was applied to fit the SAXS data from 1 wt% solutions.[11,12,18] Four terms are considered: the self-correlation of the core, the self-correlation of the corona chains, the cross term between the sphere and the corona chains, and the cross term between different corona chains.

$$P_{\mathrm{mic}}(q) = N_{\mathrm{agg}}^2\beta_{\mathrm{core}}^2A_{\mathrm{core}}^2(q) + N_{\mathrm{agg}}\beta_{\mathrm{corona}}^2P_{\mathrm{chain}}(q) + 2N_{\mathrm{agg}}^2\beta_{\mathrm{core}}\beta_{\mathrm{corona}}A_{\mathrm{core}}(q)A_{\mathrm{corona}}(q) + N_{\mathrm{agg}}(N_{\mathrm{agg}} - 1)\beta_{\mathrm{corona}}^2A_{\mathrm{corona}}^2 \quad (2)$$

Here q is the scattering vector, N_{agg} is the aggregation number, and β_{core} and β_{corona} are total excess scattering lengths of core and corona blocks, respectively. They are defined as $\beta_{\mathrm{core}} = v_{\mathrm{core\text{-}block}}(\rho_{\mathrm{core\text{-}block}} - \rho_{\mathrm{solvent}})$ and $\beta_{\mathrm{corona}} = v_{\mathrm{corona\text{-}block}}(\rho_{\mathrm{corona\text{-}block}} - \rho_{\mathrm{solvent}})$, where $v_{\mathrm{core\text{-}block}}$ and $v_{\mathrm{corona\text{-}block}}$ are the volume of the core and corona chains, calculated assuming densities of 1.047 and 0.856 g/cm^3 for PS and PEP, respectively. Also, $\rho_{\mathrm{core\text{-}block}}$, $\rho_{\mathrm{corona\text{-}block}}$, and ρ_{solvent} are the scattering length densities of the core block, corona block, and solvent, respectively.

The first term in eq 2 is the self-correlation of the spherical homogeneous core with radius R_c and a smoothly decaying scattering length density at the core-corona surface:

$$A_{\mathrm{core}}^2(q) = \Phi^2(qR_c)\exp(-q^2\sigma_{\mathrm{int}}^2) \quad (3)$$

where $\Phi(x) = 3[\sin x - x\cos x]/x^3$ is the hard-sphere form factor. The exponential term reflects a smoothly decaying density at the core-corona surface, and σ_{int} takes into account the width of the interface.

The second term in eq 2 is the self-correlation of the corona chains, which is approximated by a Debye function where the chains are considered as Gaussian chains with radius of gyration R_g:

$$P_{\mathrm{chain}}(q) = \frac{2[\exp(-x) - 1 + x]}{x^2} \quad (4)$$

with $x = q^2R_g^2$.

The last two terms in eq 2 are the cross term between core and corona and between corona chains, respectively. Both terms includes the form factor of the corona chains which is given as the normalized Fourier transform of the radial density distribution function of the corona chains, $\rho_{corona}(r)$, as follows:

$$A_{\mathrm{corona}}(q) = \frac{4\pi\int\rho_{corona}(r)\frac{\sin(qr)}{qr}r^2\mathrm{d}r}{4\pi\int\rho_{\mathrm{corona}}(r)r^2\mathrm{d}r}\exp(-q^2\sigma_{\mathrm{int}}^2/2) \quad (5)$$

In this study, a linear combination of two cubic b spline functions was chosen as $\rho_{\mathrm{corona}}(r)$, as has been successfully applied previously.[11,18] The explicit form of $\rho_{\mathrm{corona}}(r)$ is given by Bang and co-workers,[17] following the function initially developed by Pedersen and co-workers.[18] The last exponential term in eq 5 provides a smooth variation of scattering length density at the core-corona interface.

Assuming a hard-sphere structure factor, the total coherent scattering intensity is

$$I(q) = \mathrm{P}_{\mathrm{mic}}(q) + A_{\mathrm{mic}}(q)^2[S(q) - 1] \quad (6)$$

where $S(q)$ is the monodisperse hard-sphere structure factor (which depends on the hard sphere radius, R_{hs}, and the hard sphere volume fraction, η_{hs}), and $A_{\mathrm{mic}}(q)$ is the form factor amplitude of the radial scattering length distribution of the micelle given by

$$A_{\mathrm{mic}}(q) = N_{\mathrm{agg}}(\beta_{\mathrm{core}}A_{\mathrm{core}}(q) + \beta_{\mathrm{corona}}A_{\mathrm{corona}}(q)) \quad (7)$$

To account for polydispersity in micelle size, a Gaussian distribution for the core radii was used:

$$D(R_{\mathrm{c}}) = \frac{1}{\sqrt{2\pi}\sigma_R}\exp\left[\frac{-(R_{\mathrm{c}} - \langle R_{\mathrm{c}}\rangle)^2}{2\sigma_R^2}\right] \text{ for } R_{\mathrm{c}} > 0 \quad (8)$$

In this expression, $\langle R_{\mathrm{c}}\rangle$ is the average radius and σ_R is the width of the distribution, which is truncated at $R_{\mathrm{c}} = 0$. The coherent scattering intensity for the polydisperse model is then

$$I(q) = \int D(R_{\mathrm{c}})(P_{\mathrm{mic}}(\mathrm{q}) + A_{\mathrm{mic}}(q)^2[S(q) - 1])\mathrm{d}R_{\mathrm{c}} \quad (9)$$

This expression is called the local monodisperse approximation, as derived by Pedersen.[30]

In all, nine parameters could be adjusted in the fits: the core radius (R_{c}), the radius of gyration of the corona chains (R_{g}), the width of the core-corona interface (σ_{int}), the width of the distribution for the core radius (σ_R), two terms (a_1, s) in the cubic b spline function for the corona term, the hard sphere radius (R_{hs}), the hard sphere volume fraction (η_{hs}), and the aggregation number (N_{agg}). Since the SAXS data were not converted into an absolute scale, an arbitrary prefactor was introduced. The fitting range was 0.008 Å^{-1} < q < 0.11 Å^{-1}.

Results and Discussion

Hydrodynamic Radius of SEP Polymers in Squalane. The hydrodynamic radii of the four copolymers are shown as a function of temperature in Figure 2, during both heating and cooling ramps. A test sample of 0.5 wt% SEP(42−60) in squalane was prepared by dissolving the polymer in squalane with methylene chloride as a cosolvent, but without annealing at high temperature. As shown in Figure 2a, the initial room temperature R_{h} was about 650 Å, but after heating to 190 °C and cooling, the value was closer to 400 Å. Subsequent heating and cooling cycles for this polymer gave more reproducible results, with much less temperature dependence to the micelle dimensions. This initial metastable state has been reported previously with SEP in PEP-selective solvents[31,32] and interpreted in terms of kinetically frozen micelles, due both to the low critical micelle concentration (CMC) and high glass

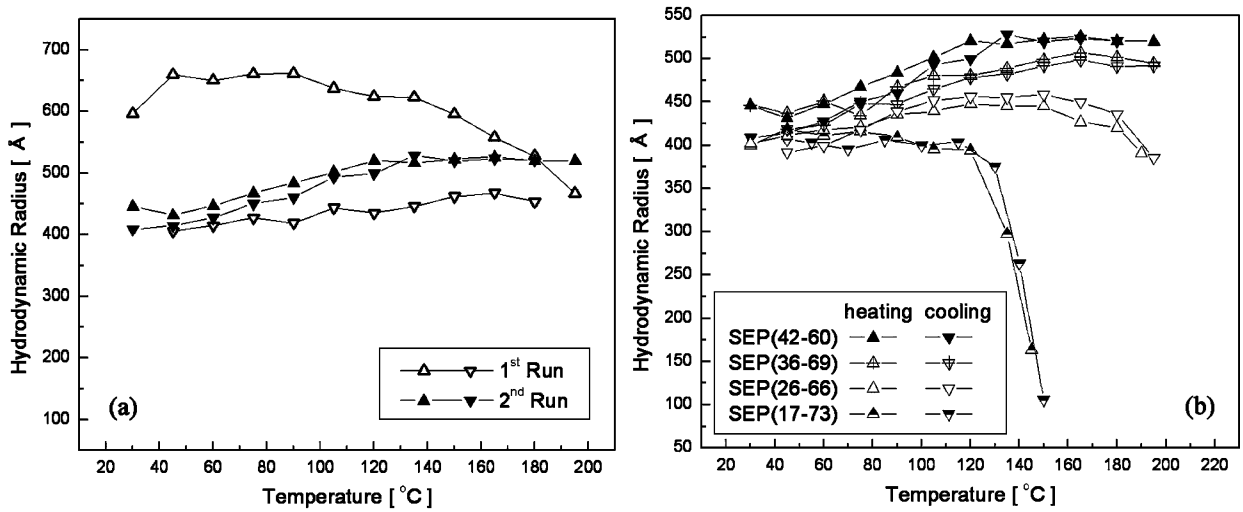

Figure 2. Temperature dependence of the hydrodynamic radius (R_h) of (a) SEP(42−60) in squalane at 0.5 wt% (R_h measured upon heating and cooling twice) and (b) all four polymers in squalane at 0.5 wt%, upon heating and cooling. Prior to the measurements in b, all samples were annealed at 190 °C for at least 15 min.

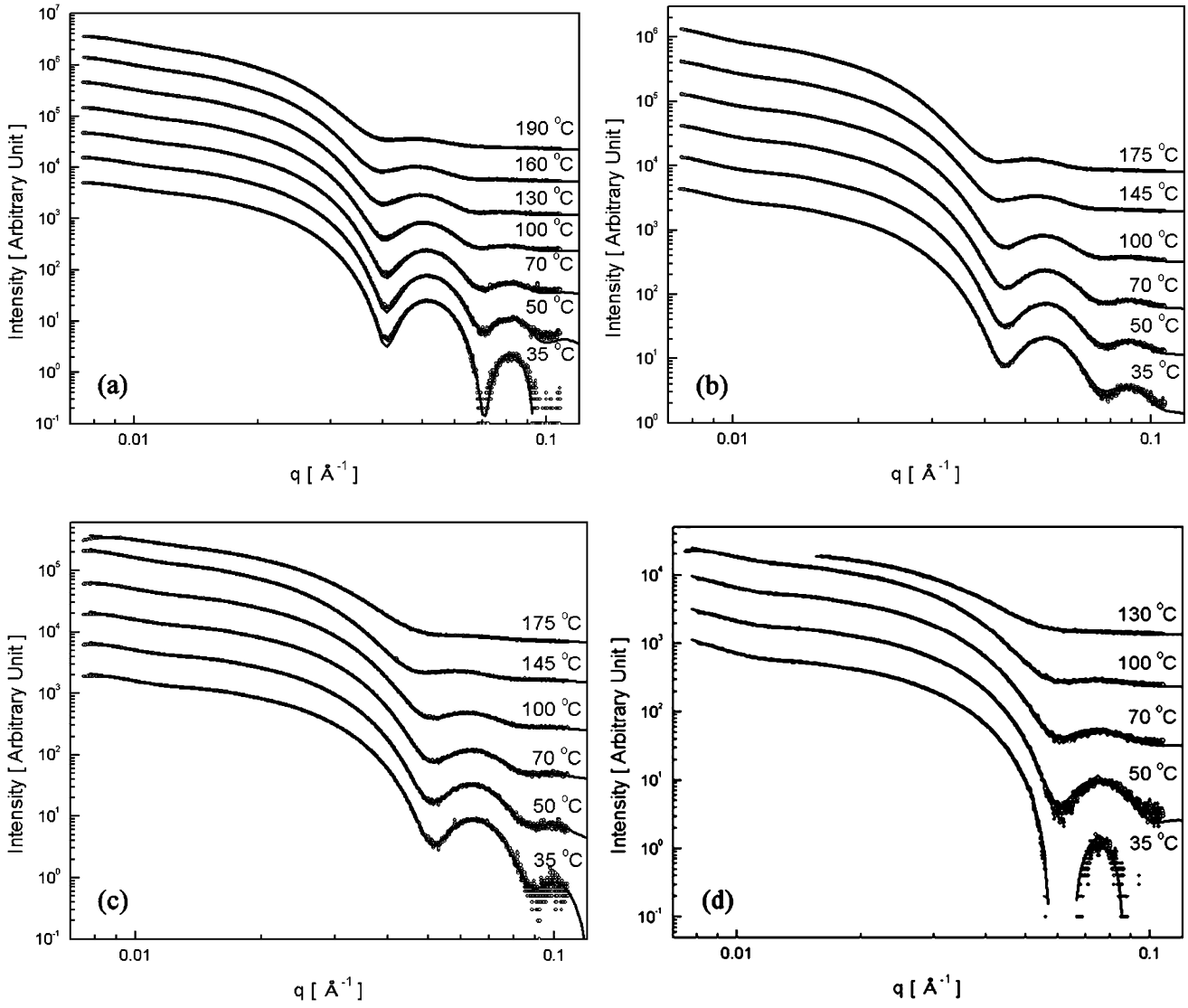

Figure 3. SAXS data upon heating for 4 SEP diblock copolymers in squalane at 1 wt%: (a) SEP(42−60), (b) SEP(36−69), (c) SEP(26−66), and (d) SEP(17−73). For clarity, data are multiplied by powers of 3 as temperature increases. The symbols are the SAXS data and the solid lines are the model fits.

transition temperature (T_g) of the core block. Thereafter, all micelle solutions were annealed at high temperature (∼190 °C) for at least 15 min before measurement. The resulting R_h of the four SEP polymer solutions as a function of temperature are

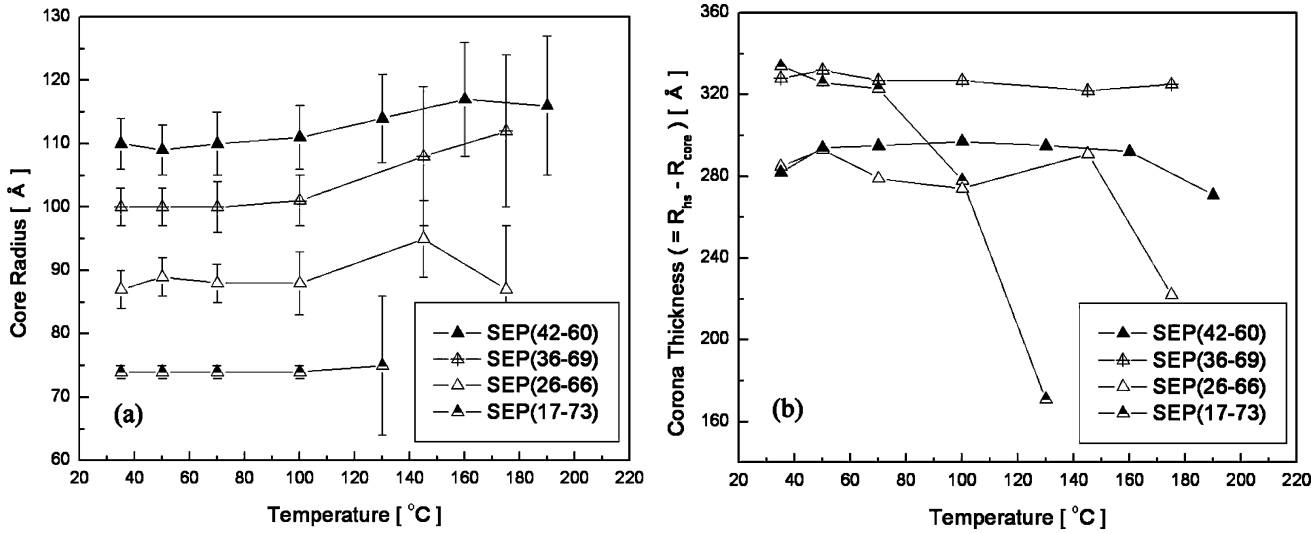

Figure 4. Temperature dependence of (a) core radius (R_c) and (b) corona layer thickness (L_{corona}) for the four polymers in squalane at 1 wt%.

TABLE 2: Fit Result upon Heating

T [°C]	R_c [Å]	N_{agg}	R_{hs} [Å]	σ_R [Å]	σ_{int} [Å]	η_{hs}
SEP(42−60) in squalane at 1 wt%						
35	110	84	392	4	9	0.05
50	109	83	404	4	10	0.06
70	110	83	404	5	11	0.06
100	111	85	407	5	12	0.07
130	114	86	409	7	12	0.07
160	117	82	408	9	12	0.07
190	116	76	386	11	11	0.05
SEP(36−69) in squalane at 1 wt%						
35	100	74	428	3	12	0.11
50	100	74	432	3	12	0.11
70	100	73	428	4	13	0.10
100	101	74	428	4	14	0.10
145	108	75	431	11	9	0.10
175	112	75	437	12	9	0.10
SEP(26−66) in squalane at 1 wt%						
35	87	68	372	3	11	0.07
50	89	71	381	3	12	0.06
70	88	69	367	3	12	0.07
100	88	70	362	5	12	0.07
145	95	75	386	6	14	0.04
175	87	58	309	10	21	0.03
SEP(17−73) in squalane at 1 wt%						
35	74	61	408	1	12	0.09
50	74	62	400	1	11	0.06
70	74	62	397	1	12	0.06
100	74	63	351	1	15	0.04
130	75	40	247	11	9	0.02

shown in Figure 2b. All four polymers have similar and constant radii up to about 60 °C. Then, R_h begins to increase slightly, before leveling off at higher temperature. The apparent increase in R_h is due at least in part to intermicellar interactions; the temperature dependence of R_h is attenuated when a more dilute solution (0.02 wt%) SEP(42−60) is examined (see Supporting Information). A critical micelle temperature (CMT) near 140 °C is evident for SEP(17−73), and a suggestion of a CMT appears for SEP(26−66) near 200 °C. The two polymers with longer polystyrene blocks do not show evidence of a CMT, because of the high incompatibility between squalane and polystyrene block. Quintana and co-workers characterized SEP micelles in *n*-alkane solvents ($n \leq 16$), and found the aggregation numbers to be constant far below the CMT, but to decrease sharply near the CMT.[25,26] This is consistent with our DLS

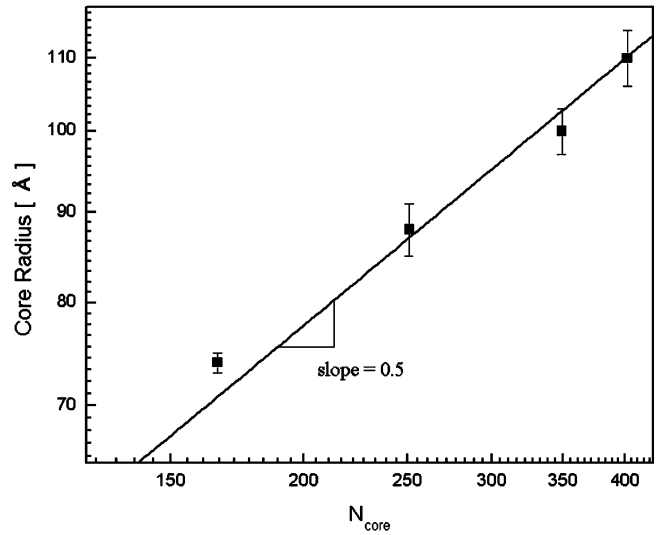

Figure 5. Relationship between the core radius and the number of repeat units in the core block.

results, and the more detailed small-angle X-ray scattering results to be described next.

Small Angle X-ray Scattering. Figure 3 displays the SAXS data for 1 wt% SEP polymer solutions measured upon heating (data obtained upon cooling are very similar, and are shown in Supporting Information). Each solution shows a distinct first minimum and maximum in the form factor at low temperature, which becomes progressively smeared out as temperature increases. Also, the position of the first minimum shifts to higher q as the molecular weight of the PS block decreases. All of the smooth curves in Figure 3 represent the best fits to the model given in the previous section, as will be discussed subsequently. As the electron density difference between PS and squalane (0.101 mol e^- cm^{-3}) is four times as large as that between PEP and squalane (0.025 mol e^- cm^{-3}), thus most of the scattering comes from the core. Consequently, the calculated scattering intensity is insensitive to variations in the three terms in eq 2 associated with the corona chains, R_g, a_1, and s, and accordingly these parameters are not reported here. The temperature dependence of the radius of the core and the corona layer thickness, which is taken as the difference between the core radius and the hard sphere radius in the structure factor, are shown in Figures 4a and b, respectively. Within the uncertainty,

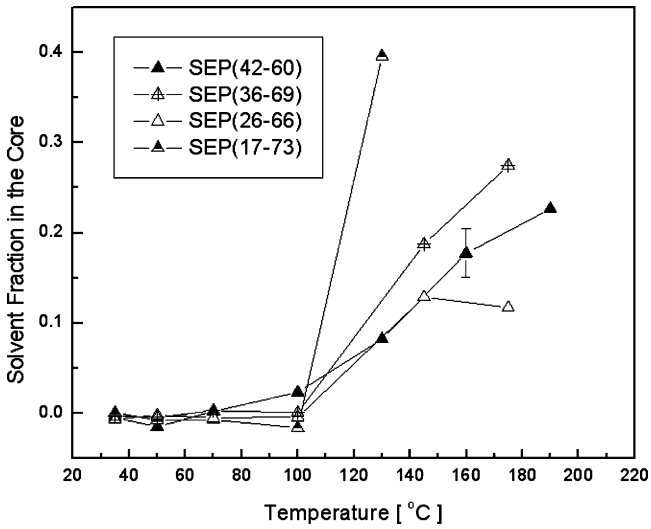

Figure 6. Temperature dependence of the solvent fraction in the core (f).

neither quantity shows any appreciable temperature dependence prior to falling off rapidly near the CMT. All of the fitting parameters are listed in Table 2.

Because of the strong core scattering, the position of the first minimum in the form factor can be used directly to extract a core size. Applying the characteristic equation for the minima in the hard-sphere form factor, $\sin(qR_c) - qR_c\cos(qR_c) = 0$, the core radius ($R_c$) at 70 °C can be estimated as 110, 102, 86, and 75 Å for SEP(42−60), SEP(36−69), SEP(26−66), and SEP(17−73), respectively, with $qR_c = 4.493$ at the first minimum. These estimated values agree well with the fitting results.

We can compare the unperturbed radius of gyration $\langle R_g\rangle_0$ of the core block to the core radius. Since the value of $6\langle R_g^2\rangle_0/MW$ is equal to 0.434 for PS at 413 K,[33] $\langle R_g\rangle_0$ of PS with 41,800, 36,300, 26,100, and 17,300 g/mol is 55, 51, 44, and 35 Å for SEP(42−60), SEP(36−69), SEP(26−66), and SEP(17−73), respectively. The fact that the core radius is only about twice $\langle R_g\rangle_0$ shows that core chains are not significantly stretched. As shown in Figure 5, R_c is roughly proportional to $N_{PS}^{0.5}$, where N_{PS} is the degree of polymerization of the core block. This is somewhat surprising, because theory anticipates significant stretching of the core blocks. For example, R_c is expected to be proportional to $N_{core}^{3/5}$ or $N_{core}^{2/3}$ for $N_{core} \ll N_{corona}$ (hairy micelles) or $N_{core} \gg N_{corona}$ (crew-cut micelles), respectively, where N_{core} and N_{corona} are the degrees of polymerization of the core block and corona block.[34,35]

Figure 6 shows the solvent fraction in the core (f), calculated by $(4/3)\pi R_c^3 = N_{agg}v_{core\text{-}block}/(1-f)$. Roughly, solvent molecules begin to penetrate into the core above 100 °C, that is, near the glass transition of the core block. Register and co-workers have reported that the glass transition temperature (T_g) of 19 kDa PS block in a PS-PI diblock copolymer is approximately 70 and 40 °C in squalane and tetradecane, respectively, in dilute solution.[21] Also Lodge and co-workers determined that the solvent fraction in the core of 30 kDa symmetric PS-PI in *n*-tetradecane is almost zero below 40 °C.[19] Therefore, it is reasonable that virtually no squalane penetration in the polystyrene core domain is observed below 70 °C. Above 100 °C, the fraction of solvent in the core increases with temperature, attributable to a decrease of the solvent selectivity for the core blocks. Nevertheless, the core size is only weakly dependent on temperature in the system, and penetration of solvent is accompanied by only small changes in aggregation number except near the CMT where the width of the core size distribution (σ_R) also rises.

As noted previously, the radius of gyration R_g of the corona chains cannot be extracted reliably from the fits, due to the small electron density difference of the corona and the solvent. In place of R_g, a corona thickness, $L_{corona} = R_{hs} - R_c$, can be used to describe the corona profile, where R_{hs} is the effective hard sphere radius in the structure factor. Roughly, R_g can be estimated as half of the corona thickness, with the assumption of nonpenetration of the corona chains into the core region. The corona layer thickness is independent of temperature between 30 and 190 °C for SEP(42−60) and SEP(36−69), where the CMT is far above the experimental range, and decreases near the CMT for SEP(26−66) and SEP(17−73) as shown in Figure 4b. Here, we can compare R_g of the corona chains to the unperturbed $\langle R_g\rangle_0$ of the corona block. Since the value of $6\langle R_g^2\rangle_0/MW$ is equal to 0.924 for *alt*-PEP at 298 K,[33] $\langle R_g\rangle_0$ of PEP with 61,800, 71,200, 68,000, and 75,200 g/mol is 98, 105, 102, and 108 Å, respectively. A dimensionless parameter s_{corona} ($\equiv R_g/\langle R_g\rangle_0$) provides a measure of corona chain stretching: s_{corona} is 1.5, 1.6, 1.4 and 1.5 for SEP(42−60), SEP(36−69), SEP(26−66), and SEP(17−73), respectively at 70 °C. As temperature approaches the CMT, the interfacial tension de-

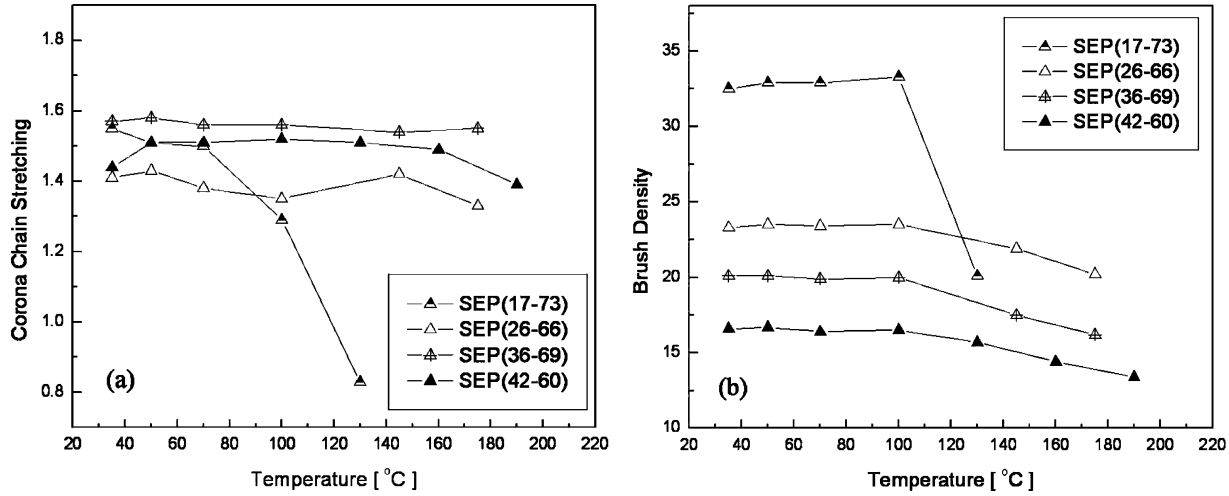

Figure 7. Temperature dependence of (a) corona chain stretching and (b) brush density for four SEP diblock copolymers in squalane at 1 wt%.

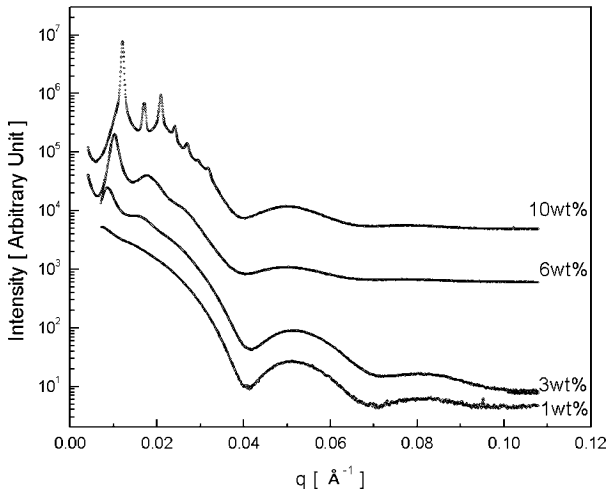

Figure 8. SAXS data of SEP(42−60) in squalane at various concentrations (1, 3, 6, and 10 wt%).

creases and both core and corona chains can relax,[19] therefore R_g approaches $\langle R_g \rangle_0$ near the CMT for SEP(17−73) as shown in Figure 7(a). The corona chains can also be characterized by the dimensionless brush density ($\equiv N_{agg}\pi\langle R_g\rangle_0^2/4\pi R_c^2$). The brush density relates the projected surface area per chain ($\pi\langle R_g\rangle_0^2$) to that available per chain on the surface of the core ($4\pi R_c^2/N_{agg}$), which is a two-dimensional analog of the reduced concentration c/c*, where c* is the overlap concentration. The brush density is 16, 20, 23, and 33 for SEP(42−60), SEP(36−69), SEP(26−66), and SEP(17−73), respectively at 70 °C. Due to the relatively high brush density, the corona chains are expected to be tightly packed and stretched out in order to reduce the number of monomer−monomer interactions. More detailed corona profiles could be acquired using small angle neutron scattering with appropriate contrast.[19]

Representative SAXS data for more concentrated solutions of SEP(42−60) at 70 °C are shown in Figure 8. At 1 wt% copolymer, clear structure factor peaks emerge at low q, which evolve into well-defined Bragg reflections from a BCC lattice by 10 wt%. The solution at 6 wt% is right on the edge of forming an ordered state. The first minimum of the form factor is found at similar q values (∼0.041 Å^{-1}) for the four different concentration samples, but the position of the first structure factor peak moves toward higher q. This suggests that the core size and aggregation number do not depend much upon polymer concentration, but the mean distance between two neighboring

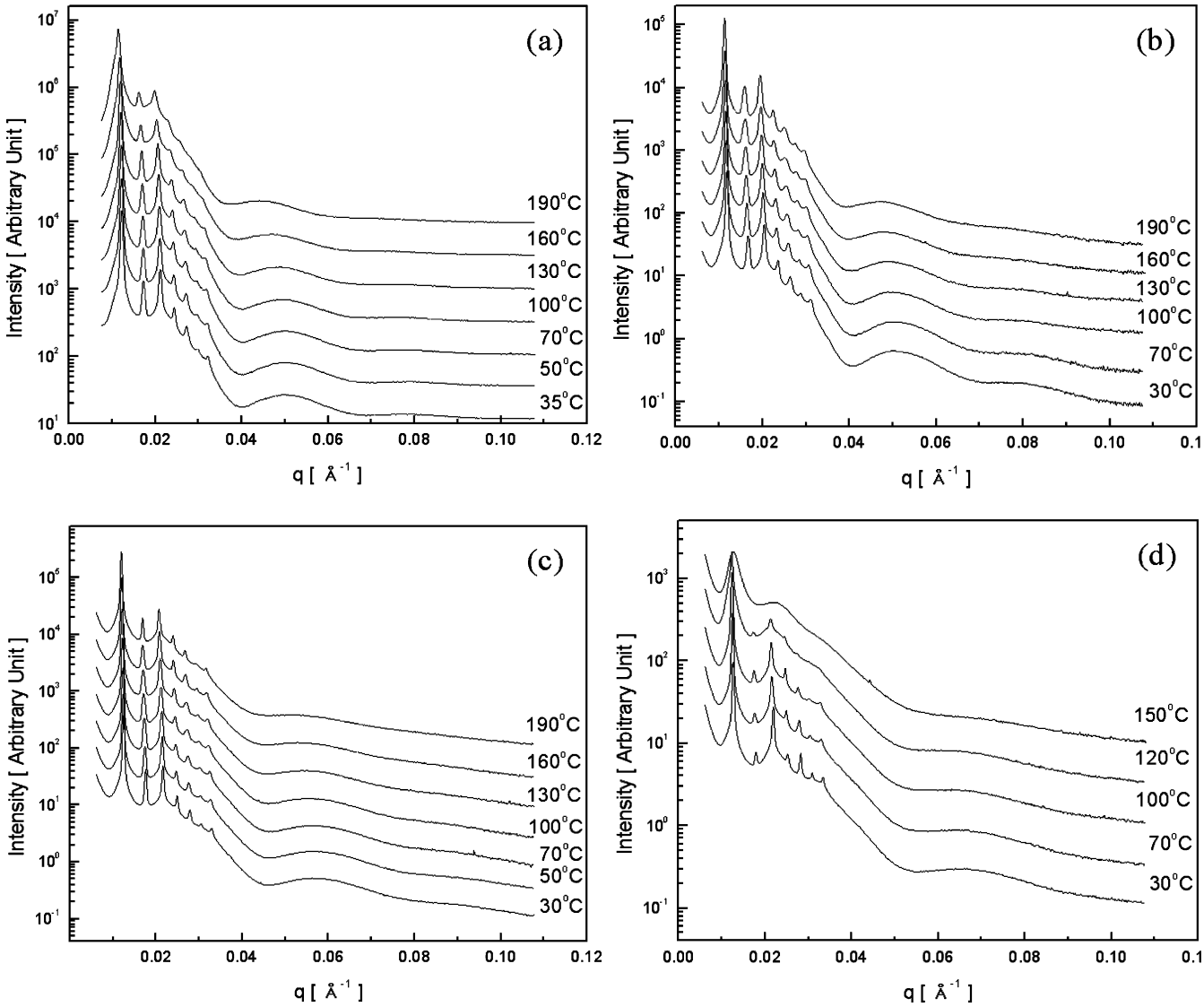

Figure 9. SAXS data of ordered SEP 10% solutions in squalane upon heating: (a) SEP(42−60), (b) SEP(36−69), (c) SEP(26−66), and (d) SEP(17−73).

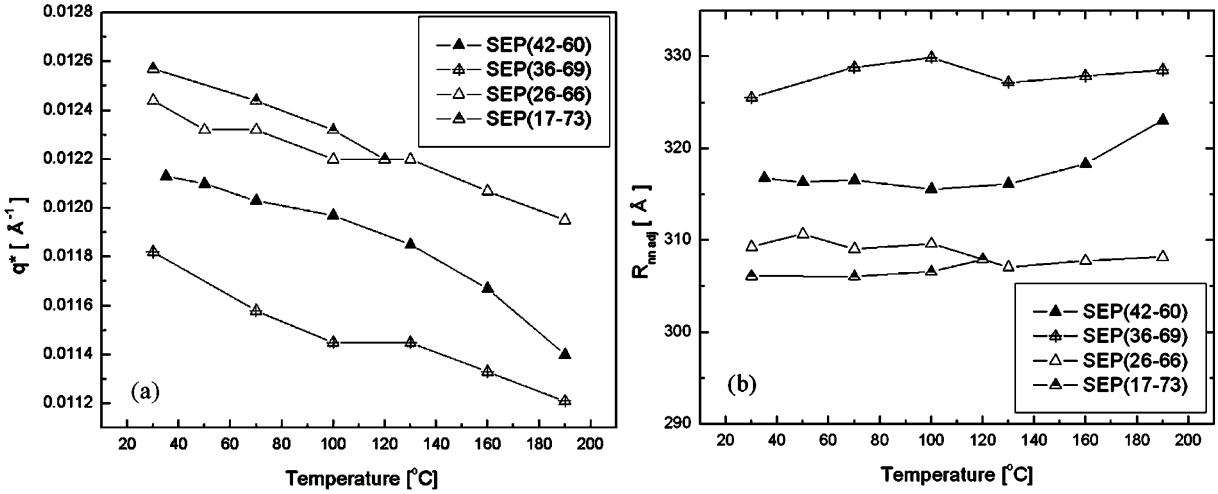

Figure 10. Temperature dependence of (a) peak position q^* and (b) the nearest neighbor radius corrected for thermal expansion, for the four SEP polymers in squalane.

cores decreases with concentration. Since the corona chains are well solvated at the periphery of the corona layer, EP blocks should be able to interpenetrate somewhat as the concentration is raised to the point of ordering, resulting in relatively "soft" intermicelle interactions.

Figure 9 shows SAXS data for 10 wt% solutions, which clearly adopt well-defined BCC lattices with peak ratios (q/q^*, where q^* is the primary peak) of $1:2^{1/2}:3^{1/2}:4^{1/2}:5^{1/2}:6^{1/2}:7^{1/2}$. Since the SEP polymers have very long corona blocks relative to the core, and the micelles interact through a "soft" potential, it is reasonable that they pack on a BCC lattice.[21,36−40] The distance between two micelles leads to a nearest neighbor radius (R_{nn}) that can be computed through the BCC lattice parameter (a_{bcc}).

$$R_{nn} = \frac{\sqrt{6}}{4}\frac{2\pi}{q^*} = \frac{\sqrt{3}}{4}a_{bcc} \tag{10}$$

As expected, R_{nn} is smaller than both R_h and R_{hs}, that is, $R_{nn} = 320$ Å relative to $R_{hs} = 405$ Å (at 1 wt%) and $R_h = 450$ Å for SEP(42−60) at 70 °C, due to corona interpenetration at higher concentration. The temperature dependence of the primary peak position q^* is shown in Figure 10a; q^* decreases smoothly with increasing temperature, except that an abrupt decrease near the CMT is observed for SEP(17−73). The corresponding R_{nn} is presented in Figure 10b, after correcting for the temperature dependence of the (solvent) density.[41] The adjusted lattice parameter is essentially independent of temperature. This is consistent with the work of Liu et al., who found that the primary peak of the BCC lattice is independent of temperature for poly(styrene-*b*-ethylene-*alt*-propylene) in squalane.[42] Note that the magnitude of R_{nn} at a given temperature varies in the sequence SEP(17−73) ≤ SEP(26−66) < SEP(42−60) < SEP(36−69), although the overall range of R_{nn} is small (<10% variation). This sequence follows the size of the core block, except for the latter two, where the longer corona block in SEP(36−69) dominates. This work contrasts with the position of the primary peak of the BCC lattice for poly(styrene-*b*-isoprene) in selective solvents, which increases with increasing temperature.[43,44] This behavior has been attributed to the decreasing solvent selectivity with increasing temperature.

Summary

In this report, the structures of poly(styrene-*b*-ethylene-*alt*-propylene) (SEP) diblock copolymers in squalane were studied. Due to the elevated glass transition temperature of the polystyrene cores, the micelles can be trapped in nonequilibrium assemblies following low temperature dispersion. Such metastable configurations were minimized by using a volatile cosolvent followed by heating to well above T_g. DLS and SAXS measurements of the resulting micellar dispersions, augmented by quantitative modeling of the latter, provides a detailed picture of micelle structure and intermicelle association as a function of block copolymer molecular weight and composition, concentration, and temperature. Selectivity of squalane for the EP corona diminishes with increasing temperature, ultimately resulting in dissolution at the highest measurement temperatures for the lowest molecular weight diblocks. This decrease in solvent selectivity leads to solvent penetration into the core resulting in a reduction in core diameter as the critical micelle temperature (CMT) is approached. An interesting conclusion drawn from our analysis is that the core blocks appear to be unstretched and that the core radius is only weakly dependent on temperature. Increasing the block copolymer concentration causes the corona chains from opposing micelles to interpenetrate. Between 6 and 10 wt%, all four SEP copolymers order on a BCC lattice. The intermicellar spacing, corrected for thermal expansion of the solution, is essentially independent of temperature. For the lowest molecular weight studied, an order-to-disorder transition occurs below 190 °C, consistent with the dilute solution CMT. Overall, these results will aid in designing complex fluids based on dispersions of diblock copolymers in hydrocarbon solvents.

Acknowledgment. This work was supported by Infineum USA L.P. The works were performed at the DuPont-Northwestern-Dow Collaborative Access Team (DND-CAT) Synchrotron Research Center located at Sector 5 of the Advanced Photon Source. DND-CAT is supported by the E.I. DuPont de Nemours & Co., the Dow Chemical Company, the U.S. National Science Foundation through Grant DMR-9304725, and the State of Illinois through the Department of Commerce and the Board of Higher Education Grant IBHE HECA NWU 96. Use of the Advanced Photon Source was supported by the U.S. Department of Energy, Basic Energy Sciences, Office of Science, under Contract No. W-31-109-Eng-38.

Supporting Information Available: ^{1}H NMR spectra and GPC traces for the four copolymers, further DLS results, SAXS data and fit parameters (Figures S1−S12, Table S1). This material is available free of charge via the Internet at http://pubs.acs.org.

References and Notes

(1) Hamley, I. W. *The Physics of Block Copolymers*; Oxford University: New York, 1998.
(2) Riess, G. *Prog. Polym. Sci.* **2003**, *28*, 1107–1170.
(3) Gohy, J.-F. *Adv. Polym. Sci.* **2005**, *190*, 65–136.
(4) Goldmints, I.; von Gottberg, F. K.; Smith, K. A.; Hatton, T. A. *Langmuir* **1997**, *13*, 3659–3664.
(5) Goldmints, I.; Yu, G.-E.; Booth, C.; Smith, K. A.; Hatton, T. A. *Langmuir* **1999**, *15*, 1651–1656.
(6) Poppe, A.; Willner, L.; Allgaier, J.; Stellbrink, J.; Richter, D. *Macromolecules* **1997**, *30*, 7462–7471.
(7) Alexandridis, P.; Yang, L. *Macromolecules* **2000**, *33*, 3382–3391.
(8) Alexandridis, P.; Yang, L. *Macromolecules* **2000**, *33*, 5574–5587.
(9) Lobry, L.; Micali, N.; Mallamace, F.; Liao, C.; Chen, S.-H. *Phys. Rev. E* **1999**, *60*, 7076–7087.
(10) Won, Y.-Y.; Davis, H. T.; Bates, F. S.; Agamalian, M.; Wignall, G. D. *J. Phys.Chem. B* **2000**, *104*, 7134–7143.
(11) Castelletto, V.; Hamley, I. W.; Pedersen, J. S. *J. Chem. Phys.* **2002**, *117*, 8124–8129.
(12) Castelletto, V.; Hamley, I. W.; Pedersen, J. S. *Langmuir* **2004**, *20*, 2992–2994.
(13) Sommer, C.; Pedersen, J. S. *Langmuir* **2005**, *21*, 2137–2149.
(14) McConnell, G. A.; Gast, A. P.; Huang, J. S.; Smith, S. D. *Phys. Rev. Lett.* **1993**, *71*, 2102–2105.
(15) McConnell, G. A.; Lin, E. K.; Gast, A. P.; Huang, J. S.; Lin, M. Y.; Smith, S. D. *Faraday Discuss.* **1994**, *98*, 121–138.
(16) Förster, S.; Wenz, E.; Lindner, P. *Phys. Rev. Lett.* **1996**, *77*, 95–98.
(17) Pedersen, J. S.; Hamley, I. W.; Ryu, C. Y.; Lodge, T. P. *Macromolecules* **2000**, *33*, 542–550.
(18) Pedersen, J. S.; Svaneborg, C.; Almdal, K.; Hamley, I. W.; Young, R. N. *Macromolecules* **2003**, *36*, 416–433.
(19) Bang, J.; Viswanathan, K.; Lodge, T. P.; Park, M. J.; Char, K. *J. Chem. Phys.* **2004**, *121*, 11489–11500.
(20) Bang, J.; Jain, S.; Li, Z.; Lodge, T. P.; Pedersen, J. S.; Kesselman, E.; Talmon, Y. *Macromolecules* **2006**, *39*, 1199–1208.
(21) Lai, C.; Russel, W. B.; Register, R. A. *Macromolecules* **2002**, *35*, 841–849.
(22) Won, Y.-Y.; Davis, H. T.; Bates, F. S. *Macromolecules* **2003**, *36*, 953–955.
(23) Jain, S.; Bates, F. S. *Macromolecules* **2004**, *37*, 1511–1523.
(24) Lund, R.; Willner, L.; Stellbrink, J.; Lindner, P.; Richter, D. *Phys. Rev. Lett.* **2006**, *96*,, 068302.
(25) Quintana, J. R.; Villacampa, M.; Muñoz, M.; Andrio, A.; Katime, I. A. *Macromolecules* **1992**, *25*, 3125–3128.
(26) Quintana, J. R.; Villacampa, M.; Andrio, A.; Muñoz, M.; Katime, I. A. *Macromolecules* **1992**, *25*, 3129–3136.
(27) Lodge, T. P.; Pudil, B.; Hanley, K. J. *Macromolecules* **2002**, *35*, 4707–4717.
(28) Hahn, S. F. *J. Polym. Sci., Part A: Polym. Chem.* **1992**, *30*, 397–408.
(29) Koppel, D. E. *J. Chem. Phys.* **1972**, *57*, 4814–4820.
(30) Pedersen, J. S. *J. Appl. Crystallogr.* **1994**, *27*, 595–608.
(31) Higgins, J. S.; Blake, S.; Tomlins, P. E.; Ross-Murphy, S. B.; Staples, E.; Penfold, J.; Dawkins, J. V. *Polymer* **1988**, *29*, 1968–1978.
(32) Hlavata, D.; Stejskal, J.; Plestil, J.; Konak, C.; Kratochvil, P.; Helmstedt, M.; Mio, H.; Laggner, P. *Polymer* **1996**, *37*, 799–805.
(33) Fetters, L. J.; Lohse, D. J.; Richter, D.; Witten, T. A.; Zirkel, A. *Macromolecules* **1994**, *27*, 4639–4647.
(34) Halperin, A.; Tirrell, M. V.; Lodge, T. P. *Adv. Polym. Sci.* **1992**, *100*, 31–71.
(35) Halperin, A. *Macromolecules* **1987**, *20*, 2943–2946.
(36) McConnell, G. A.; Gast, A. P.; Huang, J. S.; Smith, S. D. *Phys. Rev. Lett.* **1993**, *71*, 2102–2105.
(37) Lodge, T. P.; Bang, J.; Wang, X.; Brinker, K. L.; Burghardt, W. R. *Phys. Rev. Lett.* **2002**, *89*, 215505.
(38) Bang, J.; Lodge, T. P. *J. Phys. Chem. B* **2003**, *107*, 12071–12081.
(39) Bang, J.; Lodge, T. P. *Phys. Rev. Lett.* **2004**, *93*, 24570.
(40) Grason, G. M. *J. Chem. Phys.* **2007**, *126*, 114904.
(41) The density of squalane was taken as $0.98879-6.01635 \times 10^{-4}$ T, from the following reference, and a reference temperature of 30 °C was selected. Fañdino, O.; Pensado, A. S.; Lugo, L.; Comuñas, M. J. P.; Fernández, J. *J. Chem. Eng. Data* **2005**, *50*, 939–946.
(42) Liu, Z.; Shaw, M. T.; Hsiao, B. S. *J. Rheol.* **2004**, *48*, 1389–1405.
(43) Sebastian, J. M.; Lai, C.; Graessley, W. W.; Register, R. A. *Macromolecules* **2002**, *35*, 2707–2713.
(44) Lodge, T. P.; Bang, J.; Park, M. J.; Char, K. *Phys. Rev. Lett.* **2004**, *92*, 145501.

JP8111149